Journal of *Marine Science and Engineering*

MDPI

Article

A Numerical Simulation Study and Effectiveness Evaluation on the Flow Field Effect of Trapezoidal Artificial Reefs in Different Layouts

Xiaolong Chen, Xuan Che *, Yin Zhou, Changfeng Tian and Xinfeng Li

Fishery Machinery and Instrument Research Institute, Chinese Academy of Fishery Sciences, Shanghai 200092, China; chenxiaolong@fmiri.ac.cn (X.C.); zhouyin@fmiri.ac.cn (Y.Z.); tianchangfeng@fmiri.ac.cn (C.T.); lixinfeng@fmiri.ac.cn (X.L.)
* Correspondence: chexuan@fmiri.ac.cn

Abstract: The combined release of artificial reefs in different quantities and arrangements leads to different flow field effects. This study designs a small trapezoidal artificial reef. To optimize the quantity and layout of these reefs, trapezoidal reefs in three different layouts were selected for analysis at five different velocity gradients (0.1, 0.5, 1.0, 1.5, and 2.0 m/s). The effects of disposal spacing and layout on the flow field effect of trapezoidal artificial reefs at different flow velocities were simulated using Ansys Fluent. According to the findings: after simulation, flow velocity could indirectly reflect the distribution of upwelling and back eddy, the scale and strength of upwelling increased as flow velocity increased, and the back eddy showed no obvious variation with flow velocity. In transverse combination mode, both the scale and strength of the upwelling and back eddy were maximized when the reef spacing was 1.0 L; in longitudinal combination mode, upwelling and back eddy reached maximum scale and strength when the disposal spacing of the reefs was 1.5 L of a single reef. In 2020, flow mapping and fishery surveys were carried out in the engineering pilot area. The results showed that the number and species of fish populations with 1.5 L spacing in the vertical combination method were significantly higher than those in other forms, and the structure of the fish reef was stable without any flipping or sliding phenomenon. This study can provide a theoretical reference for the design and the actual deployment of artificial reefs to improve the ecological restoration of the water.

Keywords: ocean engineering; artificial reef; effect of flow field; numerical simulation; ecological restoration

Citation: Chen, X.; Che, X.; Zhou, Y.; Tian, C.; Li, X. A Numerical Simulation Study and Effectiveness Evaluation on the Flow Field Effect of Trapezoidal Artificial Reefs in Different Layouts. *J. Mar. Sci. Eng.* **2024**, *12*, 3. https://doi.org/10.3390/jmse12010003

Academic Editors: Dong-Sheng Jeng and Abdellatif Ouahsine

Received: 25 October 2023
Revised: 14 December 2023
Accepted: 15 December 2023
Published: 19 December 2023

1. Introduction

With the rapid development of urbanization in China, a lot of industrial and domestic wastewater is being discharged into the ocean, leading to serious offshore environmental pollution. At present, frequent red tides are strong signals of the impact this pollution is having. Artificial reefs can form a protective biological circle, creating a harmonious and mutually beneficial ecological environment. This will help promote biodiversity, both by circulating nutrients and by creating symbiotic relationships between different marine creatures and the environment. Artificial reefs can provide various microorganisms with substrates, forming a natural ecosystem. Upwelling, streamline flow, and eddies formed by the reef area also favor the water cycle, meaning the regional ocean environment will improve as time passes.

Artificial reefs as foundational structures have been widely used in marine ranches, which have been vigorously developed in China in recent years [1,2]. Artificial reefs are artificial constructs deployed in the corresponding sea areas, and are used to create marine ranches. This helps improve the habitat for aquatic organisms, regulates and optimizes the ocean environment, and provides marine organisms with places to forage, shelter, grow, develop, and propagate. All of this plays a role in increasing and enhancing fishery

resources [3–5]. As an effective method for protecting marine biodiversity and promoting the restoration of coastal habitats, the deployment of artificial reefs plays an important role in changing ocean flow fields. The use of artificial reefs will change the particle size distribution of marine sediments, which in turn favors the accumulation of marine organic matter [6–8].

Research has shown that the proportion of fish species (as a portion of all marine organisms) improves in sea areas where artificial reefs have been deployed. This indicates that the reefs exert a significant positive effect on the density of fishery resources [9,10]. By a process of investigation, it has been found that trapezoidal artificial reefs have a good ecological effect on shallow sea areas. These types of reef are able to change the concentration of bacterial species present in the deployment area, thus significantly reducing the abundance of sulfur-oxidizing bacteria while increasing that of *Woeseia oceani* and desulfurizing bacteria [11]. The deployment of artificial reefs will also influence the flow field of the surrounding waters and significantly change the local water flow distribution; this includes flow velocity, turbulence models, and sediment conditions, providing fish with a suitable habitat [12]. Changing the flow velocity near the reefs is an important factor in increasing the presence of fish, and is related to reef shape and layout [13]. Waters where artificial reefs are deployed are relatively shallow and located in the mixed layer of the upper ocean. The momentum, heat, and flux of material exchange are all controlled by turbulent vertical mixing at this boundary layer [14]. Therefore, investigating the flow field effect of artificial reefs is a key factor when evaluating their performance, and is one that has a direct impact on the scale of construction of artificial reefs and on their subsequent evaluation.

Many studies on the flow field effect of artificial reefs have been carried out in China and overseas [15–18], with the flow fields displaying very unsteady characteristics [19–21]. The flume experiment was first used to investigate the flow field effect of artificial reefs, and as computer technology has developed, numerical simulation has also been widely used [22,23]. Various studies have verified these results, concluding that numerical simulation can accurately reflect the flow field distribution around artificial reefs [24,25]. The flow field effect of artificial reefs is influenced by many factors, such as the structure of a single reef, the reef combination model used, and the disposal spacing [26]. The structural design of the artificial reef has a significant effect on the flow field effect of a single artificial reef, which can be effectively improved by optimizing the reef structure [27]. At present, porous trapezoidal or rectangular artificial reefs are suitable for shallow sea areas due to their good stability, high water permeability, and large effective side air volume; they also favor the survival of aquatic animals, plants, and microorganisms. The direct deployment of reefs in shallow waters will maintain a natural link to the water–sediment interface on the seabed and favor a good link to the ecological chain throughout [28]. The structure and flow field of large artificial reefs have been studied throughout the world, but the flow velocity, upwelling, and back eddy of small trapezoidal artificial reefs with different layouts and different flow velocities have not been systematically analyzed. Therefore, numerical simulations of small trapezoidal artificial reefs with different layouts are needed to reflect the effects of disposal spacing on the flow field around them. This will provide a theoretical basis for the design, actual deployment, and ecological restoration of small trapezoidal artificial reefs.

According to the characteristics of shallow waters, this paper designed a small trapezoidal artificial reef with a porous structure, suitable for use in shallow waters with small flow velocity. This reef can also generate upwelling on the approaching flow surface of the reef to transport the nutrient salts from the bottom upwards, thus promoting the mass propagation and growth of all kinds of food organisms and providing good habitats, feeding and breeding sites for fish and other organisms. Fish will also be able to cluster together to form a fishery and achieve a similar ecological effect to that provided by large reefs. This study designs a small trapezoidal artificial reef, while Ansys Fluent 2021 R1 is used as the flow field analysis software. The flow field around reefs with disposal spacing using the

ratio method is then investigated to analyze their flow field distribution characteristics. This can provide a theoretical reference for the design and the future deployment of trapezoidal artificial reefs.

2. Materials and Methods

2.1. Governing Equation

The CFD (computational fluid dynamics) method is used in this study. The compressibility of the fluid and changes in temperature are not taken into account. The governing equations include the continuity and momentum equations.

The continuity equation of fluid follows the law of conservation of mass. The equation can be expressed as:

$$\frac{\partial U_i}{\partial x_i} = 0 \tag{1}$$

where U_i is the average velocity component and x_i is the Cartesian coordinate.

The governing equation obtained according to Newton's second law is used in the flow field as the momentum equation. The momentum equation can be expressed as:

$$\frac{\partial U_i}{\partial t} + U_j \frac{\partial U_i}{\partial x_j} = -\frac{1}{\rho}\frac{\partial P}{\partial x_i} + \frac{\partial}{\partial x_j}\left[\nu\left(\frac{\partial U_i}{\partial x_j} + \frac{\partial U_j}{\partial x_i}\right)\right] - \frac{\partial \overline{u_i' u_j'}}{\partial x_j} + f_i \tag{2}$$

where t is the time, ρ is the density, P is the pressure, u_i' is the velocity fluctuations due to turbulence, ν is the kinematic viscosity, $\overline{u_i' u_j'}$ is the Reynolds stress term, f is the body force such as gravity acceleration. The Reynolds stress term is introduced in the Reynolds averaging process and is expressed as:

$$-\rho\overline{u_i{}' u_j{}'} = \mu_t\left(\frac{\partial U_i}{\partial x_j} + \frac{\partial U_j}{\partial x_i} - \frac{2}{3}\frac{\partial U_k}{\partial x_k}\delta_{ij}\right) - \frac{2}{3}\rho k\delta_{ij} \tag{3}$$

where $\mu_t = \rho C_\mu \frac{k^2}{\varepsilon}$ is the eddy viscosity; C_μ is a constant. δ_{ij} is the Kronecker delta; k is the turbulent kinetic energy.

2.2. Turbulence Model

The ocean waters are large, the flow pattern is complex, and there are more eddies, so the RNG $k-\varepsilon$ turbulence model, which is more widely used in engineering, is adopted to close the Reynolds averaged equation, and this model can effectively simulate the turbulent flow with a more homogeneous distribution and smaller turbulence structure, and it is suitable for the study of the flow field effect of the artificial fish reef body. In this model, the effects of small scales can be reflected by reflecting the small-scale effects in the large-scale motions and the modified viscosity term, so that these small-scale motions are systematically removed from the control equations. At the same time, the model takes into account the effects of eddies and low Reynolds number on turbulence, which improves the accuracy of calculations in the presence of swirling flows, and is particularly suitable for describing the environment of complex flows in the ocean with large strain rate shear flows, with swirling and separation. It satisfies the following governing equations [29]:

The transport equation for turbulent kinetic energy k is:

$$\frac{\partial(\rho k)}{\partial t} + \frac{\partial(\rho U_i k)}{\partial x_i} = \frac{\partial}{\partial x_j}\left[\left(\mu + \frac{\mu_t}{\sigma_k}\right)\frac{\partial k}{\partial x_j}\right] + P_k + P_b - \rho\varepsilon + S_k \tag{4}$$

where σ_k is the turbulent Prandtl number, P_k is the production of turbulent kinetic energy (TKE) due to average velocity gradient, P_b is the production of TKE due to buoyancy, is the dissipation rate, and S_k is the source.

The transport equation for turbulent dissipation rate ε is:

$$\frac{\partial(\rho\varepsilon)}{\partial t}+\frac{\partial(\rho U_i\varepsilon)}{\partial x_i}=\frac{\partial}{\partial x_j}\left[\left(\mu+\frac{\mu_t}{\sigma_\varepsilon}\right)\frac{\partial\varepsilon}{\partial x_j}\right]+C_{1\varepsilon}\frac{\varepsilon}{k}(P_k+C_{3\varepsilon}P_b)-C_{2\varepsilon}\rho\frac{\varepsilon^2}{k}+R_\varepsilon+S_\varepsilon \quad (5)$$

where σ_ε is the turbulent Prandtl number; S_ε is the source. $C_{1\varepsilon}$, $C_{2\varepsilon}$ are model coefficients that vary within $k-\varepsilon$ turbulence models. In Equation (5), $R_\varepsilon=\frac{C_\mu\rho\eta^3(1-\eta/\eta_0)}{1+\beta\eta^3}\frac{\varepsilon^2}{k}$, where $\eta=Sk/\varepsilon$, $S=(2S_{ij}S_{ij})^{1/2}$, $S_{ij}=\frac{1}{2}(\frac{\partial U_i}{\partial x_j}+\frac{\partial U_j}{\partial x_i})$. In the RNG $k-\varepsilon$ turbulence model, $\sigma_k=1.0$, $\sigma_\varepsilon=1.2$, $C_\mu=0.0845$, $C_{1\varepsilon}=1.42$, $C_{2\varepsilon}=1.68$, $C_{3\varepsilon}=0$, $\eta_0=4.337$, $\beta=0.012$.

In this paper, the finite volume method is used to discretize the control equations, SIMPLEC algorithm is used for pressure–velocity coupling, standard difference format is used for pressure term processing, second-order upward format is used for spatial discretization of equations, the residual value of calculation is taken to be 10^{-5}, and an unstructured mesh is used to simulate the hydrodynamic characteristics of the square reef numerically, to study the hydrodynamic characteristics of trapezoidal artificial reefs of different layout forms and its changing law under the action of different flow velocities.

2.3. Reef Model

The flow field experiment for trapezoidal reefs featured three different layouts, each of which was composed of 1 or 5 trapezoidal reefs. They refer to single reef, transverse combination reefs, and longitudinal combination reef. The reef structures are shown in Figure 1. Five actual flow velocities (0.1, 0.5, 1.0, 1.5, and 2.0 m/s) in the water were selected according to gradient designs of maximum flow velocity and experimental flow velocity in the reef-deployed waters. The specifications of the simulated reef were consistent with those of the actual model. The specific size was 0.7 × 0.5 m (length × height), with a bilateral hole diameter of 0.2 m, while the wall thickness was 0.05 m.

2.4. Computational Domain, Boundary Conditions, and Meshing

The length of the computational domain was 30 times the length of the reef, its width was 10 times the reef length, and its height was 6 times the reef length, i.e., 21 × 7 × 4.2 m (Figure 2), where the fore-reef was 10 times the reef length and the bottom of the reef overlapped with the computational domain. Firstly, it was supposed that the bottom is transverse and has not been washed over, with no need to consider the existence of creatures in other waters; secondly, it was supposed the initial flow velocity and flow direction of the incoming flow are constant; finally, it was supposed that the reef remains stable and does not roll or slide [30–32]. Velocity inlet boundary conditions were used to define the inlet boundary on the left side of the computational domain. In consideration of the average velocity conditions of the actual artificial reef-deployed waters, five water flow velocities were selected for simulation. The right side outlet boundary was set as the pressure outlet condition, while the bottom surface of the computational domain and the reef surface featured no-slip wall boundary conditions. Both side and top surfaces of the computational domain adopted symmetrical boundary conditions.

Meshing was performed on the computational domain using the Fluent Mesh module. All meshes were unstructured tetrahedral meshes. In order to increase computational accuracy, the center of the reef bottom was taken as the center; local mesh encryption was performed in the range of a circle, while the minimum mesh precision around the reef was 0.001 m, namely 1/500 of the height of the trapezoidal artificial reef. There were a total of 3.12×10^5 partitioned meshes. Meshing was shown in Figure 3. According to the calculation, the height of the first layer of the reef boundary layer is 0.002, the growth rate of the boundary layer is 1.1, and the number of layers is 12.

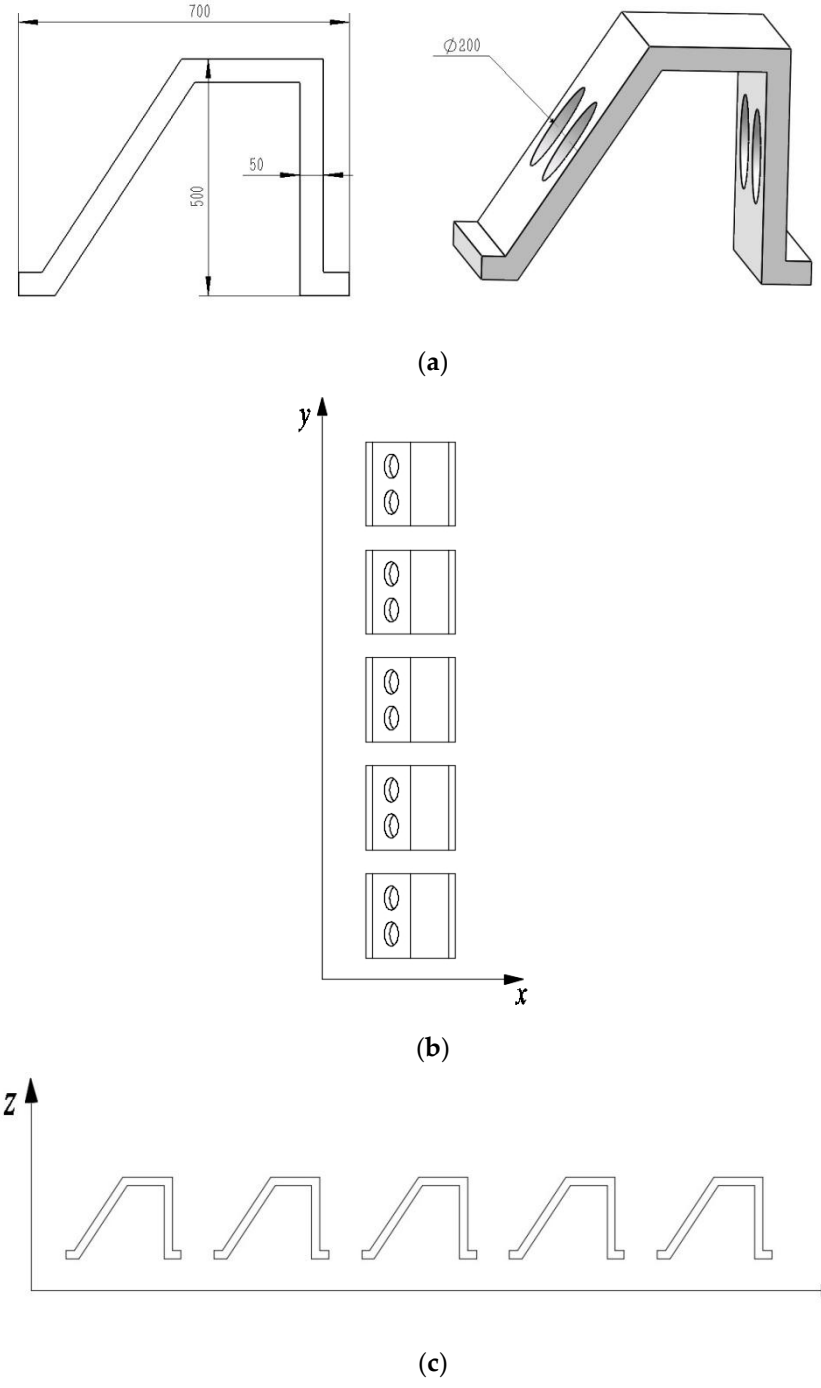

Figure 1. Models of trapezoidal reefs. (**a**) Structure of trapezoidal artificial reef. (**b**) Transverse combination. (**c**) Longitudinal combination.

2.5. Evaluation Indices and Calculation Method for Flow Field Effect

The flow field efficiency for artificial reefs was evaluated by measuring the scale of upwelling and back eddy. Researchers have found from comparative analysis of the flow field effect of commonly used artificial reefs that the difference in concrete conditions has a great effect on experimental results under the same reef height conditions. They believe that this could be used to evaluate the upwelling and back eddy effects of reefs in a more scientific and accurate manner than when using the reef volume method. In this study, upwelling and back eddy effects were evaluated by comparing the relative upwelling and back eddy volume obtained from their ratios to approaching flow volume. Therefore, the inflow direction was taken to be along the *X*-axis, while the *Z*-axis was the longitudinal

direction. X = 0 m was a mid-vertical plane; The volume on both sides of the vertical plane directly behind the artificial reef, where the ratio of the vertical upward component velocity of the *Z*-axis to the inflow velocity, being greater than 10% of the volume, was used as a measurement index for the upwelling scale. The ratio of flow velocity in the *X*-axis direction to the inflow velocity was smaller than 75% of the volume, and was used as a measurement index for the back eddy scale.

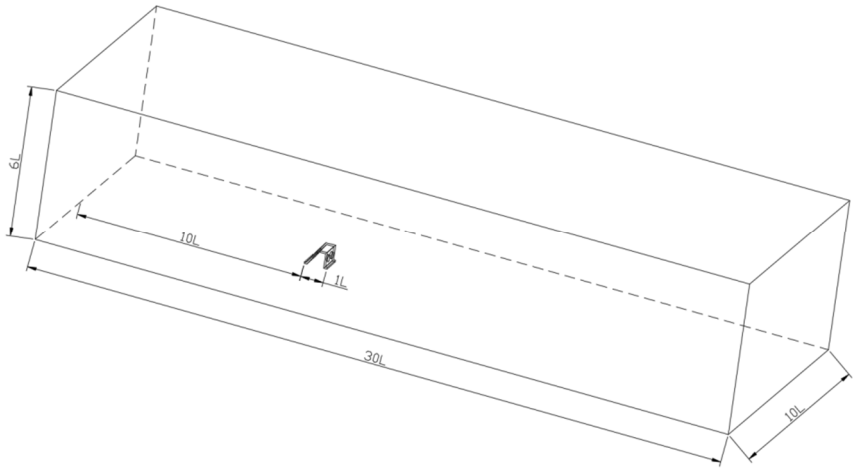

Figure 2. Computational domain of the artificial reef. Note: L is the length of reef model, 0.7 m.

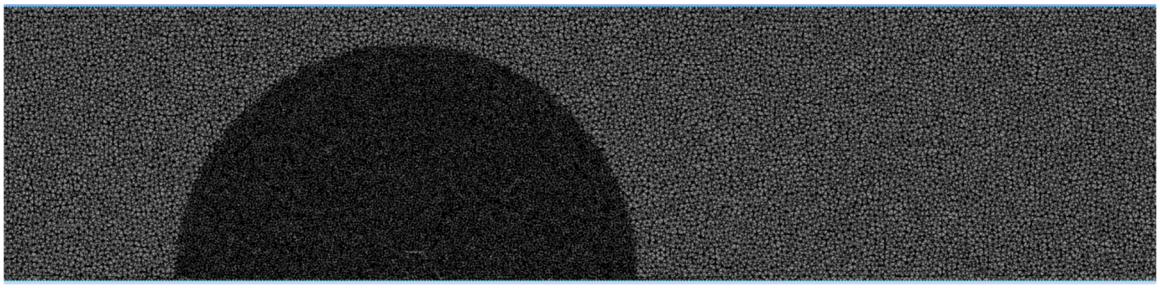

Figure 3. Meshing.

In this paper, four indexes, namely the ratio of the maximum upwelling velocity to the approaching velocity of the reef, the ratio of the upwelling height to the reef height, the ratio of the upwelling volume to the approaching volume behind the artificial reef, and the ratio of the back eddy volume to the approaching volume behind the artificial reef, are used to evaluate the strength of the upwelling and back eddy currents, which also provide a reliable method for the study of numerical simulation of artificial reefs for evaluating the effect of the flow field around the reefs.

At present, there is no agreed standard for the selection of calculation data for numerical simulation, and the selection range of this data has not been definitively described. In this study, the flow field data of three types of reefs (single reef, transverse combination reefs with a spacing of 1 L, and longitudinal combination reefs with a spacing of 1 L) at a flow approach angle of 0° and flow rate of 1.5 m/s were selected for analysis, with one datum saved every second. Based on this, a maximum upwelling velocity could be plotted (Figure 4). From Figure 4, after 63 s, it can be seen that the maximum upwelling velocity of the three types of reefs are generally stable, with no significant fluctuations. Therefore, the data selected for this study were those from the seven consecutive seconds after 63 s, which were imported into CFD-Post for averaging, after which they could undergo analysis and comparison.

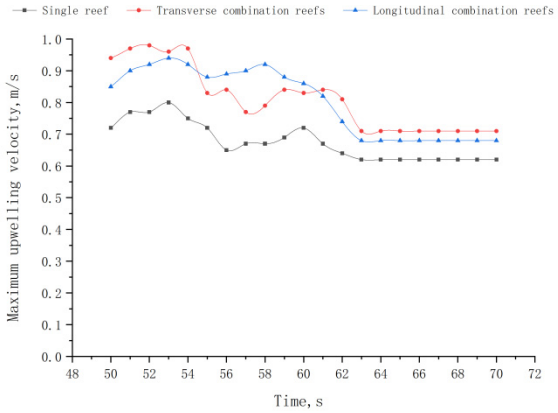

Figure 4. Upwelling volume–time curve.

3. Results and Analysis

In this study, the flow field effects of a single reef, a transverse reef combination with spacing of 0.5, 1.0, 1.5, and 2.0 L, and a longitudinal reef combination with spacing of 0.5, 1.0, 1.5, 2.0, 2.5, and 3.0 L were analyzed using the numerical simulation method, where L = 0.7 m.

3.1. Flow Field Distribution of a Single Trapezoidal Reef

In order to verify the effectiveness of the numerical simulation and testing of artificial reefs, a flume was used to test a single artificial reef, and the test results and numerical simulation results of the reef flow velocity of 1.0 m/s are shown in Figure 5. According to the above comparison results, it can be seen that the numerical model established in this paper obtained by the measurement point flow velocity and the physical model of the artificial reef experiments coincide with the results, which strongly proves that the method of this paper is selected to establish a numerical computational model to carry out the study of the dynamic characteristics of artificial reefs under the action of the water flow is feasible.

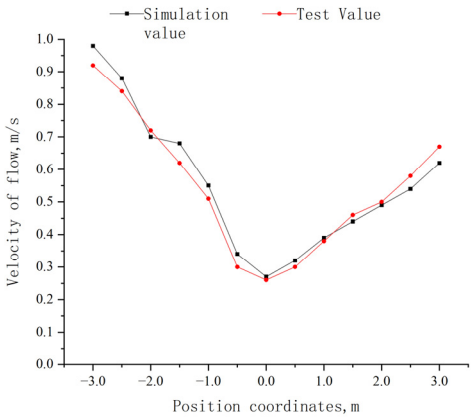

Figure 5. Comparison of simulated and experimental values of flow velocity at the measuring point.

(1) Analysis of upwelling characteristics. Figure 6a–c show the scale and strength of the upwelling of a single trapezoidal reef. It can be seen from the figures that the maximum upwelling velocity, the ratio of upwelling height to reef height, and the ratio of upwelling volume to approaching flow volume all increase as the flow velocity increases. The maximum upwelling velocity increases most rapidly; the upwelling height and volume increase slightly, while the ratio of the upwelling volume to the approaching flow volume ranges from 0.60 to 0.85; the upwelling height increases more rapidly as the flow velocity increases from 1.0 to 1.5 m/s.

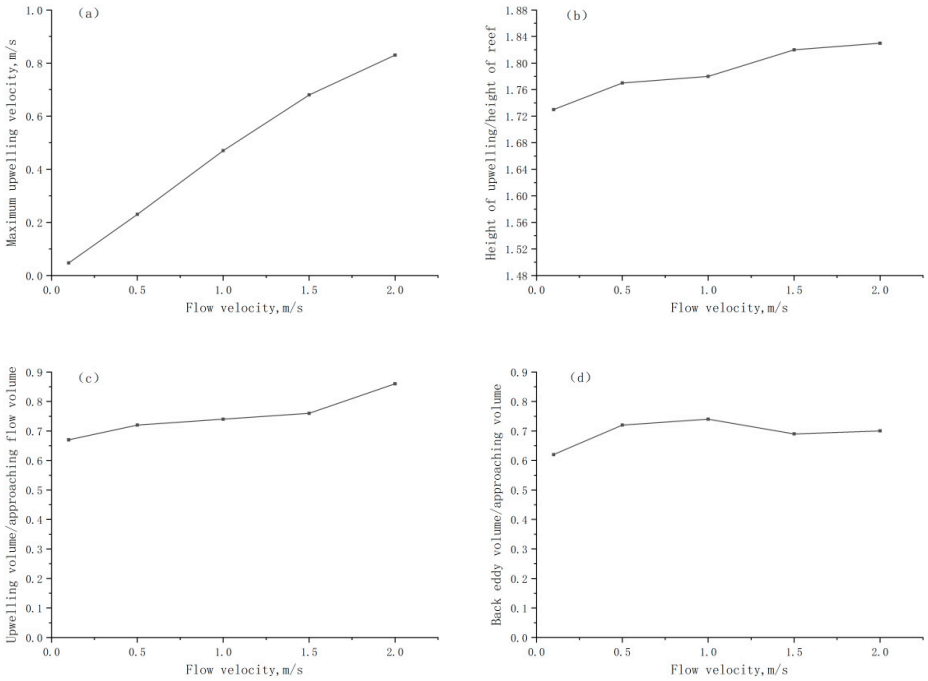

Figure 6. Scale and strength of upwelling and back eddy of a single trapezoidal reef at different flow velocities. (**a**) The variation curve of maximum upwelling velocity with flow velocity. (**b**) The variation curve of height of upwelling with flow velocity. (**c**) The variation curve of upwelling volume with flow velocity. (**d**) The variation curve of back eddy volume with flow velocity. Note: approaching volume refers to the volume of flow velocity in the *X*-axis direction.

(2) Analysis of back eddy characteristics. Figure 6d shows the scale and strength of the back eddy of a single three-round-pipe reef. It can be seen from the figure that the back eddy volume shows a tendency to increase, decrease, and then increase again as the inlet velocity increases; this reaches a maximum when the flow velocity is 1.0 m/s, before it decreases again. Generally speaking, though, it shows an increasing trend.

3.2. Effect of Transverse Combination Spacing on Flow Field around the Trapezoidal Reef

Figure 7 shows the numerical simulation results of flow field effect in a transverse combination of reefs with different disposal spacing at five different flow velocities. Each index changes as follows: As the disposal spacing increases, the maximum upwelling velocity, upwelling height, and upwelling volume show a tendency to first increase and then decrease, reaching their maximum values at a spacing of 1.0 L. The maximum upwelling velocity and upwelling height also show an insignificant tendency to increase at first and then decrease under low-velocity constraint conditions. The back eddy volume also reaches a maximum at a spacing of 1.0 L, but does not change significantly with increased disposal spacing, approximating the same back eddy volume as that of a single reef. At a given disposal spacing, and as flow velocity increases, the maximum upwelling velocity, upwelling height, and upwelling volume increase gradually, with the upwelling volume showing a consistent change trend with the single reef; the back eddy volume does not display any obvious change trend. In the transverse combination mode, the scale and strength of the upwelling and back eddy were greatest at a reef spacing of 1.0 L, meaning the maximum scale and strength of the upwelling and back eddy were obtained when the disposal spacing between two unit reefs was 1.0 L.

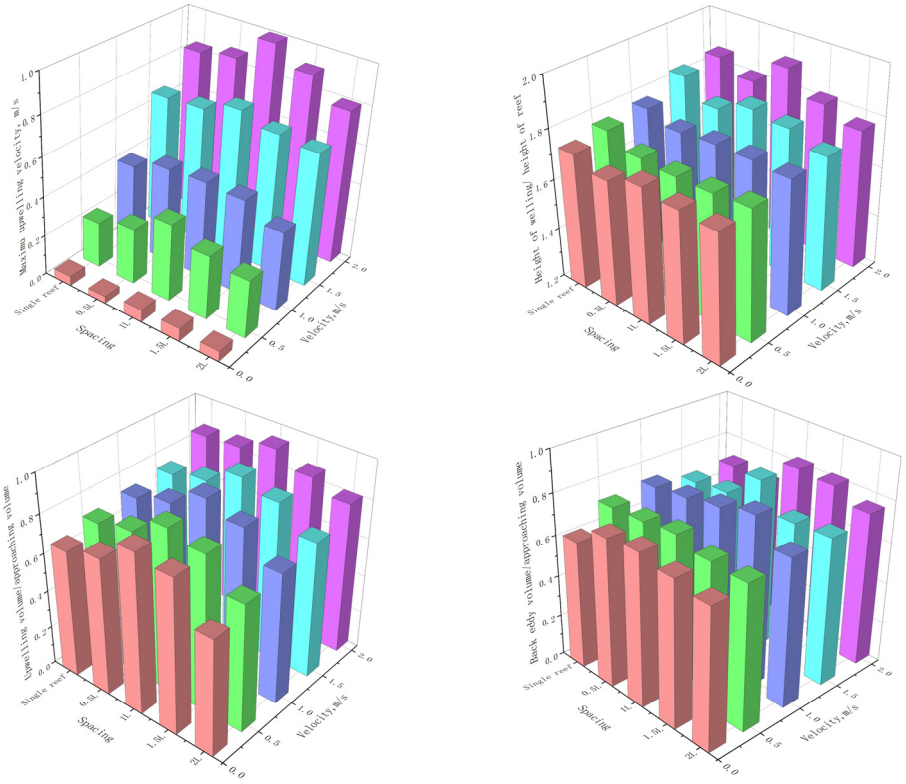

Figure 7. Scale and strength of upwelling and back eddy on trapezoidal reefs with transverse combination spacing at different flow velocities.

3.3. Effect of Longitudinal Combination Spacing on Flow Fields around the Trapezoidal Reef

Figure 8 shows the numerical simulation results for the flow field effect in a longitudinal combination of reefs with different disposal spacing at five different flow velocities. Each index changes as follows: At a given flow velocity, and as disposal spacing increases, the maximum upwelling velocity, upwelling height, and upwelling volume all show a tendency to increase at first and then decrease, reaching their maximum values at a spacing of 1.5 L. The upwelling volume shows a relatively flat tendency, with a consistent change trend for a single reef that reaches a maximum at a spacing of 1.5 L. The back eddy volume behind the reef is smaller than that of a single reef, because the sheltering effect of the front reef leads to a significant reduction in the function of the one behind. At a given disposal spacing, and as flow velocity increases the maximum upwelling velocity, the ratio of upwelling height to reef height and the ratio of upwelling volume to approaching flow volume also increase gradually, showing a consistent change trend with the single reef; the back eddy volume does not show any obvious change trend. In longitudinal combination mode, the scale and strength of the upwelling reached a maximum at 1.5 L; the scale of the back eddy on the second unit reef was significantly smaller than that for the first reef. This is possibly because the first unit reef weakens the back eddy on the second one; this means that a longitudinal layout has a large influence on the back eddy.

3.4. Stability Analysis of Trapezoidal Reefs

In order to stabilize the reef in the water, current force conditions on the different combinations of trapezoidal reef models were tested by means of model simulation. Pressure distribution of a trapezoidal reef under the impact of water flow. According to the results obtained, the maximum pressure of the trapezoidal reef is 985 Pa, and the overall flow pressure is calculated as F by the computer. The current forces for the reef model at five inflow velocities, specific flow velocities, and force conditions under various working conditions are shown in Table 1.

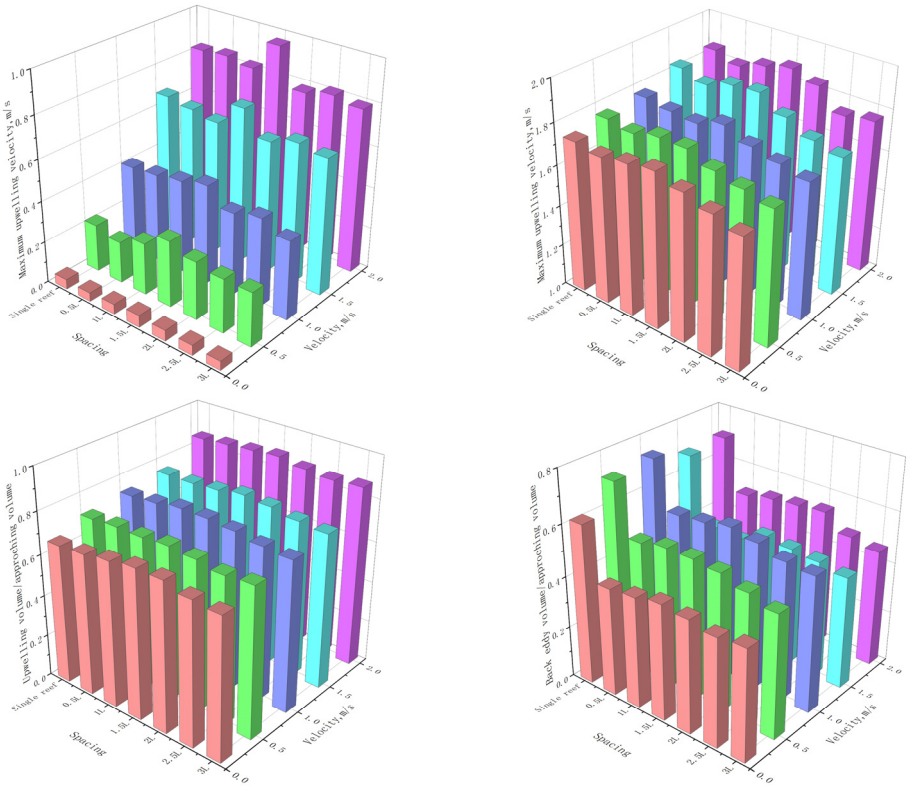

Figure 8. Scale and strength of upwelling and back eddy of trapezoidal reefs with longitudinal combination spacing at different flow velocities.

Table 1. Current forces exerted on the model at five flow velocities.

	1	2	3	4	5
Flow velocity, m/s	0.1	0.5	1.0	1.5	2.0
Current force, KN	0.0368	0.0435	0.0546	0.0767	0.0979

3.4.1. Analysis of Anti-Slide Safety

For the reef not to slide, the maximum static frictional force between reef and seabed must be greater than the fluid force exerted on the reef itself, and the anti-slide coefficient $S_1 > 1$. The calculation is as follows:

$$S_1 = \frac{W_\mu(1-\rho/\sigma)}{F_{max} > 1} \tag{6}$$

where W is the weight of the trapezoidal reef model, 1.0916 KN; μ is the maximum static friction coefficient using the particle size for medium sand (0.60); ρ is the water density, 1025 kg/m^3; σ is the weight of the reef per unit volume, 2500 kg/m^3; and F is the current force exerted on the reef. The analytical calculation results are shown in Table 2.

Table 2. Stability analysis for the reef model at five different flow velocities.

	1	2	3	4	5
Flow velocity, m/s	0.1	0.5	1.0	1.5	2.0
Current force, KN	0.0368	0.0435	0.0546	0.0767	0.0979
Anti-slide coefficient S_1	10.50	8.88	7.08	5.04	3.95
Anti-rolling coefficient S_2	15.31	12.95	10.32	7.35	5.76

3.4.2. Analysis of Anti-Roll Safety

For the reef not to roll, the resulting moment M_1 of the gravity and buoyancy of the reef must be greater than the maximum moment M_2 of fluid force exerted upon it, and the anti-rolling coefficient $S_2 > 1$. The calculation is as follows [27]:

$$S_2 = \frac{M_1}{M_2} = \frac{W(1-\rho/\sigma)l_w}{F_{\max}h_0} \quad (7)$$

where W is weight of the trapezoidal reef model, 1.0916 KN; ρ is the water density, 1025 kg/m^3; σ is the weight of the reef per unit volume, 2500 kg/m^3; l_w is the horizontal distance between the center of gyration and the center of gravity, 0.035 m; h_0 is the height of the fluid force, 0.0400 m; and $F_{\max}$ is the current force exerted on the reef. Analytical calculation results are shown in Table 2.

According to the findings of the force analysis of the reef model under different working conditions, the current force exerted on the reef increases as the inflow velocity increases. Its stability also decreases accordingly, but as a whole, the anti-slide coefficient and anti-rolling coefficient of the reef at different flow velocities are all greater than 1. That is to say, the reef model is able to maintain its stability in the currents and waves without sliding or rolling, indicating that the reef model has a reliable structure.

4. Discussion

This study took a trapezoidal reef as an example. A comparative analysis was conducted on changes in flow field around reefs with different disposal spacing based on the Fluent numerical simulation method, after which an analysis was carried out on the stability of the reef model in the currents.

To verify the reliability of the numerical simulation method and calculations, the flow velocity of the longitudinal dam body within the ecological engineering restoration area of the Yangtze River estuary was measured in September 2020. I used the LinkQuest ADCP (San Diego, CA, USA) Doppler flow velocity meter to map the flow velocity and flow pattern around the artificial reef in the artificial reef placement area, which can measure the flow velocity and direction of each vertical point of the cross section in the watershed, with an accuracy of 0.01 m/s, and analyze and obtain the maximum upwelling flow velocity according to the previous criteria on the definition of the upwelling. The experimental results show that the longitudinal artificial fish reef has a relatively small flow velocity, significant changes in direction, and complex flow patterns. Analytical calculation results are shown in Table 3. Comparing and analyzing the experimental test results with the numerical calculation results in Table 1, it can be seen that the simulation results are basically consistent with the surveying results, with an error of less than 10%, indicating the effectiveness and high accuracy of the simulation of artificial fish reef flow patterns.

Table 3. Comparison between simulation and test data of upwelling velocity of an artificial reef.

Velocity of Flow/(m·s^{-1})	Maximum Upwelling Velocity Simulation Value/(m·s^{-1})	Maximum Upwelling Velocity Test Value/ (m·s^{-1})	Error Analysis of Flow Velocities/%
0.1	0.047	0.051	8.5
0.5	0.230	0.215	6.5
1.0	0.470	0.434	7.6
1.5	0.680	0.619	8.9
2.0	0.830	0.872	5.1

The simulation results show that, in the transverse combination mode, the scale and strength of the upwelling and back eddy were greatest at a reef spacing of 1.0 L, meaning the maximum scale and strength of the upwelling and back eddy were obtained when the

disposal spacing between two unit reefs was 1.0 L. In longitudinal combination mode, the scale and strength of the upwelling reached a maximum at 1.5 L; the scale of the back eddy on the second unit reef was significantly smaller than that for the first reef. This is possibly because the first unit reef weakens the back eddy on the second one; this means that a longitudinal layout has a large influence on the back eddy. This is basically consistent with Liu et al. [29], who analyzed the maximum change of the flow field when the model spacing is between 1.0 and 1.5 L. However, because they only analyzed the change characteristics of the flow field, without detailed analysis of the upwelling velocity and the volume of the upwelling, they were unable to judge the scale of the upwelling of the artificial reefs, and they also did not analyze the different velocities, which could not accurately respond to the characteristics of the upwelling at different velocities and under different layouts. Zheng et al. [25] also simulated the flow field effects of three stacked forms of circular tube-type artificial reefs numerically. When the number of stacked reefs is fixed, the maximum upwelling velocity and upwelling area increase with the increase in approaching velocity, which is consistent with the conclusion of this paper, but there is no analysis of the back eddy. As the simulation is mainly used to evaluate the maximum upwelling flow velocity and upwelling area, the simulation error value is around 20%, which is a large error, and at the same time, their study did not analyze the layout spacing and flow velocity of the artificial reefs, and the effect of the reefs was not investigated practically, so that the ecological significance of the reefs could not be determined. Liu et al. [17] also simulated and analyzed porous square-shaped artificial reefs, but only analyzed the height and area of the upwelling region of a single reef, with a large error value, and did not quantitatively and in detail analyze the strength of upwelling changes under different reef layouts and velocities. Yang et al. analyzed the effect of different fabrication methods on the flow field of permeable artificial reefs, but the evaluation method was simpler and did not analyze the strength of upwelling under different layouts, while the experimental results were not verified. In this study, we analyzed small trapezoidal reefs and applied the ratio method to compare the flow field effects under different velocities and different layouts, and the results had small errors, which can provide valuable references for the placement and design of artificial reefs. And stability analysis was conducted on the trapezoidal artificial reef model. It was found that it is able to maintain its stability in currents and waves, meaning stability risks are relatively low for the transverse and longitudinal reef combinations discussed in this study. This finding is of great significance for the actual planning and deployment of artificial reefs.

The survey and monitoring of the project area was carried out in September of the year before and after the ecological restoration project and at the same location according to the principle of spatial and temporal unity, and in terms of fish species, gillnets with the same mesh size of 40 mm were used to catch fish in the area where the artificial reefs were put in, as shown in Figure 9. The results showed that the number of fish species in the project area were from 40 to 49 after the construction of artificial fish reefs. Fish density is mainly used to assess the number of fish, with the American Bio Sonics DT-X (Seattle, WA, USA) finding that echo sounders (split beam, detection distance: 0.5–500 m, echo detection limit: −140 dB, sounding frequency: 0.01–30 times/second, pulse frequency: 0.1–1 milliseconds, dynamic range: more than 160 dB) are used to detect fish in the longitudinally combined artificial reef waters before and after the completion of the project; the fish density was about 0.314 fish per m^2 before the project. After the completion of the project, a fish echo detector was used to detect the fish density within the engineering area. The results showed that the fish density after the project construction was about 1.197 fish per m^2 after the construction; the fish density after project completion was about four times that before the restoration. The results are shown in Figure 9. This is mainly because the construction of artificial fish reefs changed the flow characteristics and produced more eddies, with significant changes in flow patterns and gradients, and allowed fish species to spawn in faster-flowing areas and rest and feed in still-water areas after spawning. Artificial fish reef construction provided better conditions for fish habitats. In summary, it was found that the

fish species and quantities in the test area increased during these investigations, indicating that the longitudinally combined trapezoidal artificial reefs have a very good impact on the recovery of fishery resources. This study can thus provide a theoretical basis for the design, deployment, and ecological restoration in waters featuring trapezoidal artificial reefs. Figure 10 shows the trapezoidal artificial reef deployed on site.

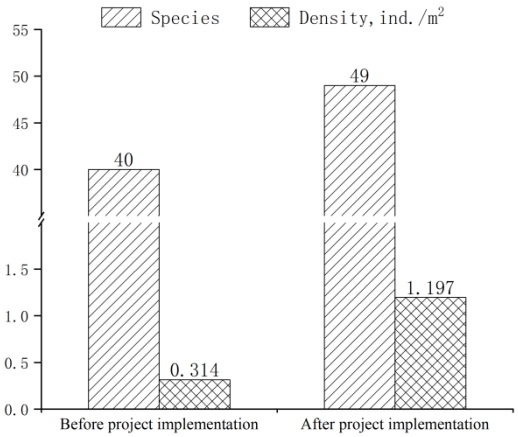

Figure 9. Comparison of fish before and after the implementation of the project.

Figure 10. Artificial reef before deployment.

5. Conclusions

This paper uses numerical simulation to simulate the strength of upwelling and back eddy around the flow field of small trapezoidal reefs under different deployment spacing and velocities, and compares and analyzes the optimal spacing of reefs under different velocities using the ratio method, and compares the results with the existing research results, which shows that the numerical simulation can better respond to the influence of the deployment spacing on the effect of the flow field around the trapezoidal reefs, and makes the analysis of the physical stability, which can provide a certain theoretical basis for the layout of artificial reefs in the actual sea area. This paper also investigates and analyzes the ecological benefits of the reefs, and the results also show that the trapezoidal reefs under this layout have better stability and ecological benefits, and also provide valuable references for the placement and design of artificial reefs.

This study analyzed the flow field effects of trapezoidal reefs under different flow velocities and spacing using numerical simulation and field survey methods. However, the flow field of reefs with different layouts was not verified in the experiments. Additionally, no optimization or improvement was made to the structure of the trapezoidal reefs, and there was no comparative analysis with other artificial reefs. In future research, it is necessary to conduct field verification experiments for reefs with different layouts and optimize the structure of trapezoidal reefs to provide a basis for their design and selection.

Author Contributions: Conceptualization, X.C. (Xiaolong Chen) and X.C. (Xuan Che); methodology, X.C. (Xiaolong Chen) and X.C. (Xuan Che); software, X.C. (Xiaolong Chen) and X.L.; validation, C.T. and Y.Z.; writing, X.C. (Xiaolong Chen). All authors have read and agreed to the published version of the manuscript.

Funding: This study was supported by Science & Technology Fundamental Resources Investigation Program (Grant No. 2022FY100404).

Data Availability Statement: The data presented in this study are available on request from the corresponding author.

Conflicts of Interest: The authors declare no conflict of interest.

References

1. Wang, H.; Chen, P.; Zhang, S.; Jia, X. Effect on fishery resources multiplication of artificial reefs. *Guangdong Agric. Sci.* **2009**, *8*, 18–21.
2. Gao, Y.; Chen, X.; Meng, S.; Hu, G.; Li, D.; Qiu, L.; Song, C.; Fan, L.; Xu, H.; XU, P. Research Progress of Artificial Reef Construction and Its Mechanism. *Chin. Agric. Sci. Bull.* **2023**, *39*, 138–144.
3. Yang, H. Construction of marine ranching in China: Reviews and prospects. *J. Fish. China* **2016**, *40*, 1133–1140.
4. Wang, Y.; Guo, D. Design and construction of marine ranch in my country. *China Fish.* **2011**, *4*, 25–27.
5. Pan, P. Marine ranch: Carrying new hope for China's fishery transformation. *China Fish.* **2016**, *1*, 47–49.
6. Yu, L. Study on Topography and Hydrodynamic Characteristics of Typical Spawning Grounds of Four Great Fishes in the Middle Reaches of the Yangtze River. Ph.D. Thesis, Southwest University, Chongqing, China, 2018.
7. Zhang, J.; Che, X.; Jiang, G.; Tian, C.; Chen, X. Effects of artificial dams on hydrodynamic characteristics of fish habitat in the upper reaches of the Yangtze River. *Chin. Soc. Agric. Eng.* **2021**, *5*, 140–146.
8. Fan, J.; Chen, P.; Feng, X.; Chen, G. Research Progress on hydrodynamics of artificial reefs. *Guangdong Agric. Sci.* **2013**, *2*, 185–188.
9. Yang, Y.; Yan, Z.; Qiao, Y. Characterization and review of hydraulic conditions of river fish habitat. *J. Hohai Univ. (Nat. Sci.)* **2007**, *2*, 125–130.
10. Sun, Y.; Niu, T.; Wang, Y.; Wang, R.; Guo, X. Simulation and restoration design of fish habitat based on terrain remodeling. *Environ. Ecol. Three Gorges* **2015**, *37*, 29–32.
11. Sun, J. Simulation of Fish Habitat in Heishui River, a Backwater Tributary of Baihetan Reservoir. Master's Thesis, Zhejiang University, Hangzhou, China, 2013.
12. Wu, J.; Wu, Z. Turbulence field of spur dike and its engineering significance. *J. Zhengzhou Inst. Eng.* **1994**, *2*, 22–27.
13. Jiang, Z. Numerical Simulation of Hydrodynamics for Artificial Reefs. Ph.D. Thesis, Ocean University of China, Qingdao, China, 2009.
14. Zhang, S.; Sun, M.; Chen, Y. Quantitative analysis of upwelling current features ofa artificial concrete reef with different height. *J. Dalian Fish. Univ.* **2008**, *23*, 353–358.
15. Pan, L.; Lin, J.; Zang, S. A numerical experiment of the effects of artificialreef on vertical 2-dimensional steady flow field. *J. Shanghai Fish. Univ.* **2005**, *14*, 406–412.
16. Li, J.; Zhang, S. The comparison between numerical simulation and water channel experiment on an Mi-zi artificial reef. *J. Fish. China* **2010**, *34*, 1587–1594. [CrossRef]
17. Liu, Y.; Guan, C.; Zhao, Y.; Cui, Y.; Dong, G. Experimental study on two-dimensional flow field of the star artificial reef in the water stream with PIV. *Chin. J. Hydrodyn.* **2010**, *25*, 777–783.
18. Guan, C.; Liu, Y.; Zhao, Y.; Cui, Y.; Li, J. Experimental study on two dimensional flow field of the compound Martificial reef with Particle Image Velocimetry (PIV). *Fish. Mod.* **2010**, *37*, 15–19.
19. Liu, Y.; Guan, C.; Zhao, Y. Numerical simulation and PIV study of unsteady flow around hollow cube artificialreef with free water surface. *Eng. Appl. Comput. Fluid Mech.* **2012**, *6*, 527–540.
20. Jiang, Z.; Liang, Z.; Tang, Y. Numerical simulation and experimental study of the hydrodynamics of a modeled reef located within a current. *Chin. J. Oceanol. Limnol.* **2010**, *28*, 267–273. [CrossRef]
21. Yakhot, V.; Orzag, S. A Renormalization group analysis of turbulence: Basic theory. *J. Sci. Comput.* **1986**, *1*, 3–11. [CrossRef]
22. Yu, D.; Yang, Y.; Li, Y. Research on hydrodynamic characteristics and stability of artificial reefs with different opening ratios. *Period. Ocean Univ. China* **2019**, *49*, 128–136.
23. Wang, J.; Liu, L.; Cai, X. Numerical simulation study on influence of disposal space on effects of flow field around porous square artificial reefs. *Prog. Fish. Sci.* **2020**, *41*, 40–48.
24. Wang, F. *Computational Fluid Dynamics Analysis*; Tsinghua University Press: Beijing, China, 2004; pp. 113–143.
25. Zheng, Y.; Liang, Z.; Guan, C. Numerical simulation and experimental study on flow field of artificial reefs in three tube-stacking layouts. *Oceanol. Limnol. Sin.* **2014**, *45*, 11–19.
26. Liu, H.; Ma, X.; Zhang, S.; Yu, H.; Huang, H. Research on model experiments of effects of artificial reefs on flow field. *J. Fish. China* **2009**, *33*, 229–236.

27. Guan, C.; Li, M.; Heng, Y.; Li, J.; Cui, Y.; Li, Z.; Wang, T. Numerical Simulation of Disposal Space and Analysis on Physical Stability of Three-Tube Artificial Reefs. *Periddical Ocean Univ. China* **2016**, *46*, 9–17.
28. Cui, Y.; Guan, C.; Wan, R. Numerical simulateon on influence of disposal space on effects of flow field around artificial reefs. *Trans. Oceanol. Limnol.* **2011**, *51*, 59–65.
29. Liu, H.; Ma, X.; Zhang, S.; Lin, j.; Yu, H.; Huang, H. Validation and comparison between wind tunnel experiments and numerical simulation of flow field around artificial reefs. *J. Fish. Sci. China* **2009**, *16*, 365–371.
30. Huggins, D.; Piedrahita, R.; Rumsey, T. Analysis of sediment transport modeling using computational fluid dynamics (CFD) for aquaculture raceways. *Aquac. Eng.* **2004**, *31*, 277–293. [CrossRef]
31. Huggins, D.; Piedrahita, R.; Rumsey, T. Use of computational fluid dynamics (CFD) for aquaculture raceway design to increase settling effectiveness. *Aquac. Eng.* **2005**, *33*, 167–180. [CrossRef]
32. Jiang, Z.; Liang, Z.; Liu, Y. Particle image velocimetry and numerical simulations of the hydrodynamic characteristics of an artificial reef. *Chin. J. Oceanol. Limnol.* **2013**, *31*, 949–956. [CrossRef]